

Review

A Review of Deep Learning Imaging Diagnostic Methods for COVID-19

Tao Zhou ^{1,2} , Fengzhen Liu ^{1,*}, Huiling Lu ³ , Caiyue Peng ¹ and Xinyu Ye ¹¹ School of Computer Science and Engineering, North Minzu University, Yinchuan 750021, China² Key Laboratory of Image & Graphics Intelligent Processing of State Ethnic Affairs Commission, North Minzu University, Yinchuan 750021, China³ School of Science, Ningxia Medical University, Yinchuan 750004, China

* Correspondence: liufengzhen2022@163.com

Abstract: COVID-19 (coronavirus disease 2019) is a new viral infection disease that is widely spread worldwide. Deep learning plays an important role in COVID-19 images diagnosis. This paper reviews the recent progress of deep learning in COVID-19 images applications from five aspects; Firstly, 33 COVID-19 datasets and data enhancement methods are introduced; Secondly, COVID-19 classification methods based on supervised learning are summarized from four aspects of VGG, ResNet, DenseNet and Lightweight Networks. The COVID-19 segmentation methods based on supervised learning are summarized from four aspects of attention mechanism, multi-scale mechanism, residual connectivity mechanism, and dense connectivity mechanism; Thirdly, the application of deep learning in semi-supervised COVID-19 images diagnosis in terms of consistency regularization methods and self-training methods. Fourthly, the application of deep learning in unsupervised COVID-19 diagnosis in terms of autoencoder methods and unsupervised generative adversarial methods. Moreover, the challenges and future work of COVID-19 images diagnostic methods in the field of deep learning are summarized. This paper reviews the latest research status of COVID-19 images diagnosis in deep learning, which is of positive significance to the detection of COVID-19.

Keywords: deep learning; COVID-19 datasets; supervised learning; semi-supervised learning; unsupervised learning



Citation: Zhou, T.; Liu, F.; Lu, H.; Peng, C.; Ye, X. A Review of Deep Learning Imaging Diagnostic Methods for COVID-19. *Electronics* **2023**, *12*, 1167. <https://doi.org/10.3390/electronics12051167>

Academic Editor: Gabriella Olmo

Received: 13 January 2023

Revised: 17 February 2023

Accepted: 23 February 2023

Published: 28 February 2023



Copyright: © 2023 by the authors. Licensee MDPI, Basel, Switzerland. This article is an open access article distributed under the terms and conditions of the Creative Commons Attribution (CC BY) license (<https://creativecommons.org/licenses/by/4.0/>).

1. Introduction

In December 2019, coronavirus disease 2019 (COVID-19) was discovered in Wuhan, China and spread rapidly around the world. COVID-19 is characterized by strong infectivity, rapid transmission and high mortality. Patients with COVID-19 mainly present with symptoms such as fever, dry cough and malaise in the early stages and severe cases present with respiratory distress, which may develop into respiratory organ failure and lead to death [1]. As of 21 July 2022, the World Health Organization (WHO) reported, 504,079,039 confirmed cases with 6,204,155 deaths [2]. Figure 1 shows the top 30 countries with the highest number of confirmed cases and deaths cases of COVID-19, where the horizontal axis represents different countries and the vertical axis represents the number of confirmed cases and deaths cases.

X-ray images (X-ray) and computed tomography images (CT) have become an important tool for the detection of COVID-19. The images of COVID-19 contain ground-glass opacities (GGOs), areas of consolidation and a mix of both in all lung lobes [3]. Figure 2 shows the X-ray and CT images of COVID-19, pneumonia and normal lungs.

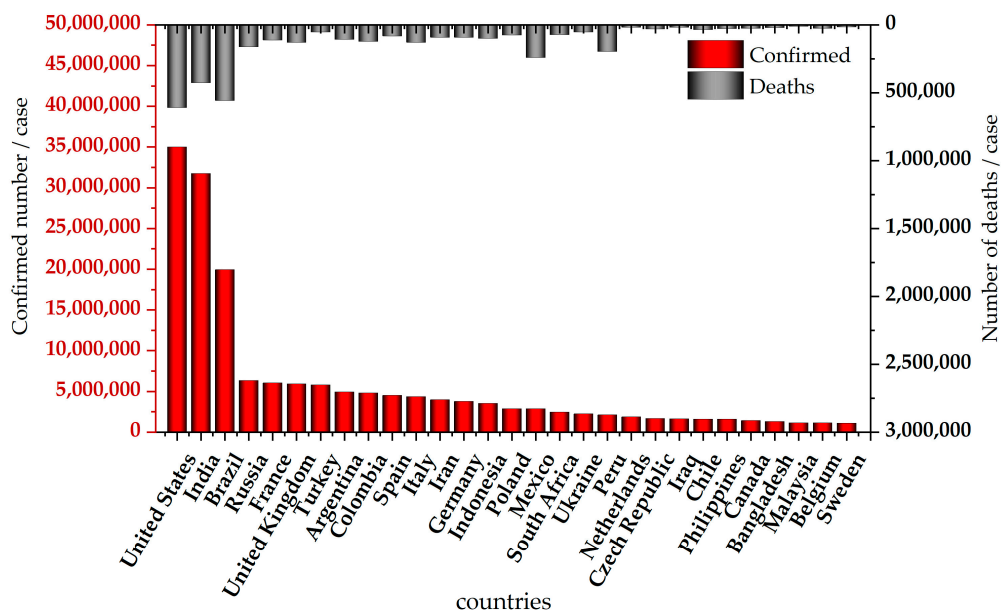


Figure 1. The number of confirmed cases and deaths cases.

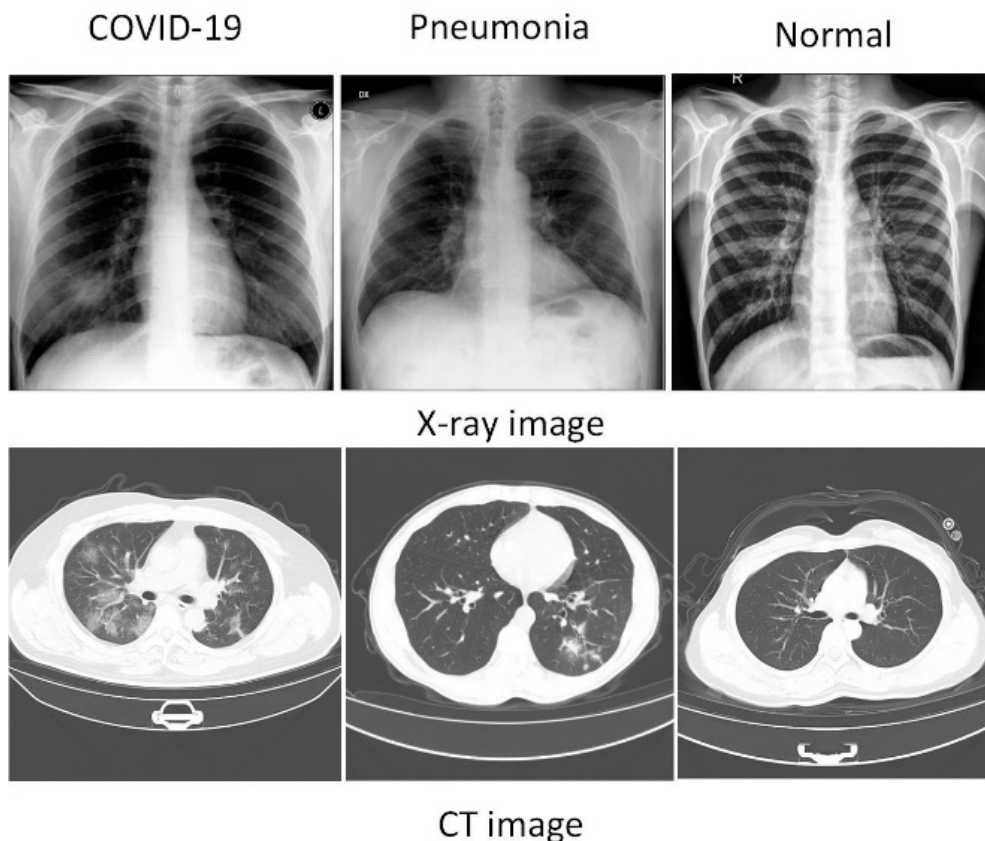


Figure 2. The X-ray and CT images of COVID-19.

Deep learning, as a powerful tool to assist physicians in diagnosis, is widely used in computer-aided diagnosis of COVID-19. This paper summarizes the application of deep learning in COVID-19 diagnosis from three aspects of supervised learning, semi-supervised learning and unsupervised learning. Supervised learning means that the model learns the association between the input and output, based on the given sample which with the corresponding label. Song et al. [4] proposed a supervised learning model for diagnosing

COVID-19 using CT images, which achieves features with a high recognition rate by feature parsimony. Ahmed et al. [1] detected COVID-19 by a supervised learning approach using a model combining preprocessing techniques and an attention module. Semi-supervised learning refers to making full use of the unlabeled samples of the dataset and automatically exploits the unlabeled samples to improve the learning performance [5]. Wang et al. [6] proposed a semi-supervised network to segment COVID-19 infected lesions, which uses a reweighting loss and a small sample iterative segmentation framework. Unsupervised learning refers to learning some useful patterns from unlabeled samples without the help of artificially given labels. Chen et al. [7] proposed an adaptive COVID-19 segmentation model to improve the performance by an unsupervised adversarial training scheme and encouraging the segmentation network to learn domain invariant features.

Deep learning methods have been widely used to assist in the diagnosis of COVID-19 images. Several review articles on COVID-19 have been published. Soomro et al. [8] summarize an extensive review of the efficient AI-based methods for efficient COVID-19 diagnosis. The review summarized the COVID-19 diagnostic methods in the aspects of classification and segmentation, which neglected the detailed summary and analysis of the existing COVID-19 datasets. A COVID-19 CT image diagnosis method based on supervised and weakly supervised learning are reviewed by Haseeb et al. [9]. However, the article does not summarize the application of X-ray images in COVID-19 deep learning model and does not summarize the application of unsupervised learning methods of COVID-19. Nandhini et al. [10] provide a review of deep learning-based detection methods for COVID-19 from transfer learning and fine-tuning, novel architectures, and other approaches. The reader can obtain the current status of research on X-ray and CT images of COVID-19, but only the classification methods used for COVID-19 are summarized and the authors provide seven COVID-19 datasets, which is not enough to illustrate the development of COVID-19 datasets.

To sum up, we can obtain a lot of knowledge about COVID-19 research status from the existing surveys. Based on the shortcomings of the existing surveys, our review provide a more comprehensive review of deep learning imaging diagnostic methods for COVID-19 from multiple perspectives. To provide readers with the latest research fields and research directions, the motivation and contribution of this paper are as follows:

1. This review provides a more comprehensive review of classification and segmentation method on CT and X-ray datasets of deep learning imaging diagnostic methods for COVID-19.
2. This review provides a comprehensive summary of the available COVID-19 datasets.
3. The advantages and challenges of deep learning imaging diagnostic methods for COVID-19 are given from multiple perspectives.

In this paper, the literature is searched through ScienceDirect, Web of Science, IEEE Xplore Digital Library, SpringerLink, and ArXiv. The CT and X-ray datasets of COVID-19 are mainly summarized from the searched literature and the Kaggle website. The keywords used in the process of searching the literature are COVID-19, deep learning, CT, X-ray, classification, segmentation, semi-supervised learning and unsupervised learning.

The main contents of this paper are organized as follows: the general architecture of the deep learning COVID-19 images diagnosis method is shown in Figure 3. Section 2 summarizes the datasets of COVID-19. Section 3 summarizes the application of deep learning methods for supervised learning in diagnosis of COVID-19. Section 4 summarizes the application of deep learning methods with semi-supervised learning in diagnosis of COVID-19. Section 5 summarizes the application of deep learning methods for unsupervised learning in diagnosis of COVID-19. Section 6 summarizes the challenges faced and future trends of deep learning in the field of COVID-19 diagnosis.

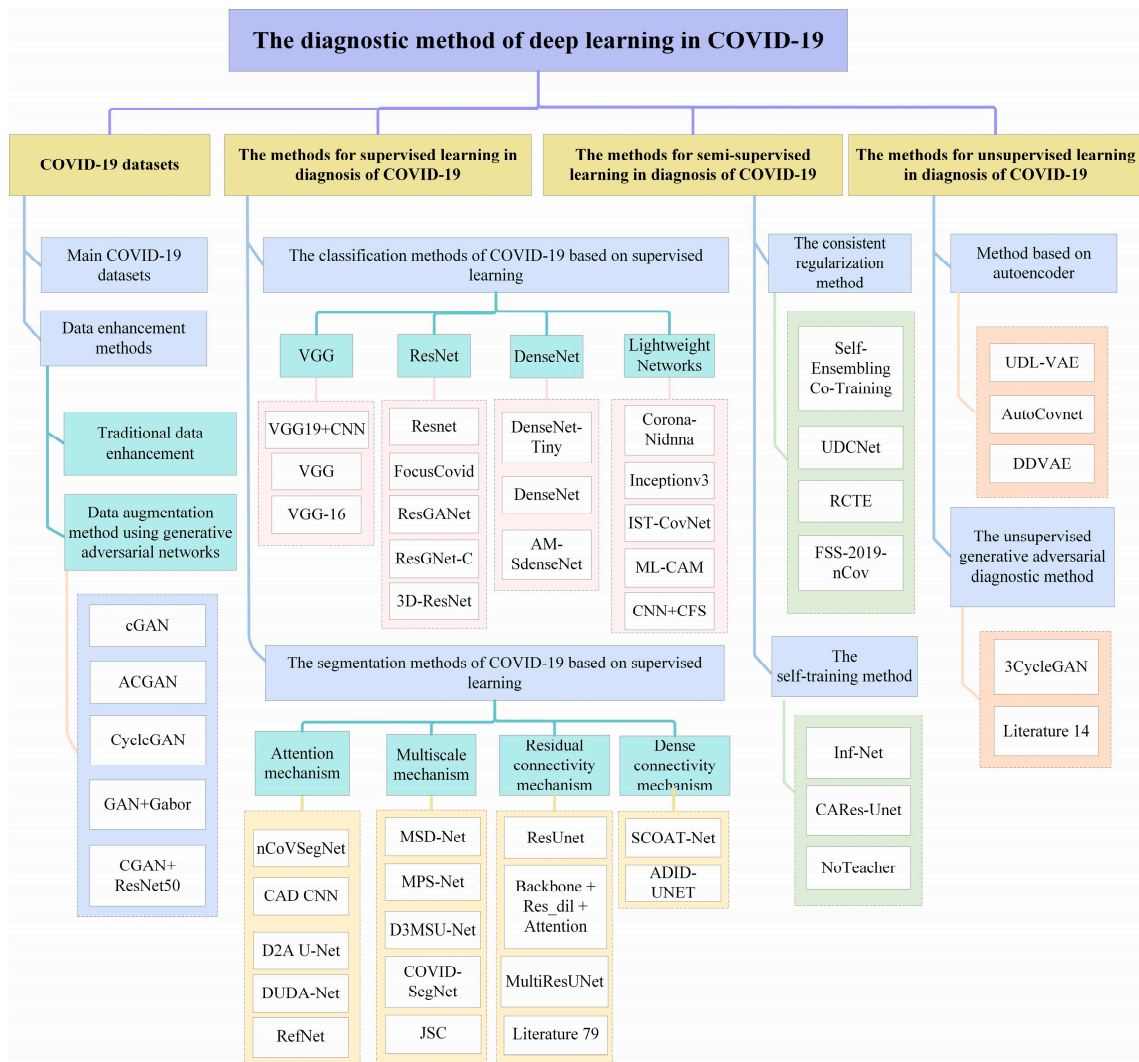


Figure 3. General architecture of deep learning COVID-19 images diagnosis method.

2. COVID-19 Datasets

The Researchers have successively released a large number of COVID-19 datasets for deep learning model training to improve the identifying ability of COVID-19 diagnostic models since the outbreak of COVID-19 in December 2019. In this section, the typical COVID-19 datasets are summarized as shown in Figure 4, which is labeled by month in order from left to right. X-ray and CT are the main types of COVID-19 datasets. The COVID-19 datasets for the X-rays modalities released from 2020 to 2022 are distributed at the top of the timeline and the COVID-19 datasets for the CT modalities released from 2020 to 2022 are distributed at the bottom of the timeline. It is easy to see that the relevant datasets were mainly released in 2020 and the CT modal COVID-19 dataset is the mainstream of the COVID-19 dataset.

2.1. Main COVID-19 Datasets

Deep learning model training requires datasets with large scale and high quality to achieve better generalization capability. In this section, the details of the COVID-19 dataset are summarized and the specific analysis is as follows, from seven aspects in the Table 1. Firstly, there are 11 COVID-19 datasets about X-ray modal, 20 about CT modal and 2 about combined X-ray and CT datasets. The CT modal dataset is more used in the COVID-19 images diagnostic study. Second, there are a total of 31 unimodal datasets and a total of

2 bimodal datasets. The unimodal dataset is mainly used in COVID-19 diagnostic study. Third, there are different sizes of COVID-19 datasets. The smaller dataset, the COVID chest X-ray dataset [11], contains 123 X-ray images and was the first X-ray dataset on COVID-19 to be publicly available, released by Cohen in February 2020. COVID-CT [12] contains 349 of COVID-19 CT images and 397 of NO-COVID-19 CT images which is the first CT dataset on COVID-19 to be publicly available. COVIDx CT-2A [13] is one of the largest and most diverse publicly available datasets, containing 194,922 CT images from 3745 individuals. COVIDx-CT [13] is a CT dataset collected by the National Center for Biological Information in China, which contains 104,009 images from 1489 patients. Fourth, COVID-19, pneumonia and normal lung are the three main types of diagnosis. Most of the COVID-19 datasets contain two of these types and multi-classified datasets are relatively rare. Fifth, the COVID-19 datasets were mainly published by researchers or institutions in China, Canada and Italy, of which the number of the researchers who contributed to the COVID-19 datasets were 14, 4, 3. Sixth, there is a difference in the density of datasets released in different time periods. The number of datasets published in 2020 is more than that in 2021, including 21 in 2020, 8 in 2021, 2 in 2022. In 2020, the most intensive three months of datasets release are April, May and June, with a total of 9 datasets released. Finally, the formats of JPG and PNG plays a main role in the type of JPG, JPEG, PNG DICOM, NIFIT and CKPT on COVID-19 datasets.

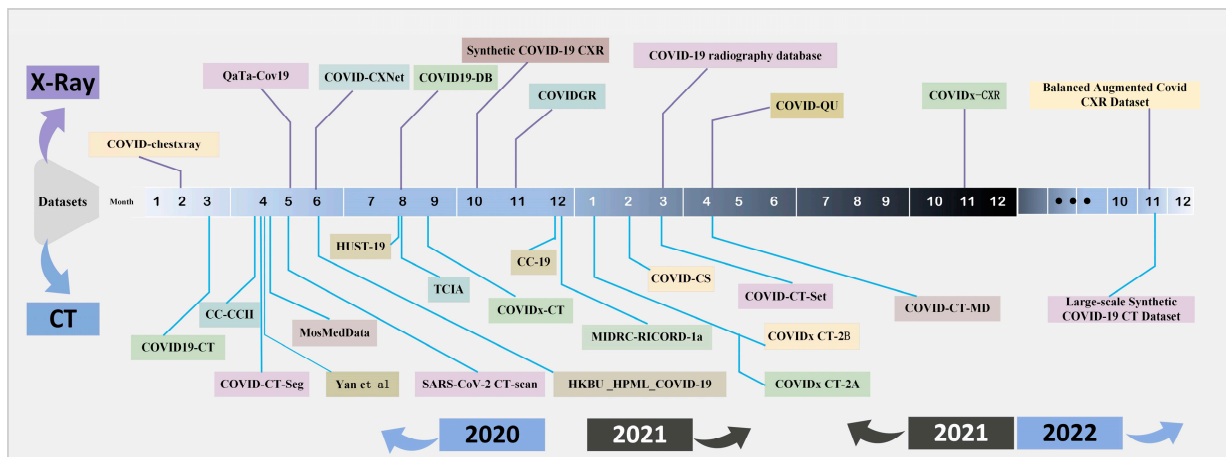


Figure 4. COVID-19 dataset.

Table 1. COVID-19 public datasets.

| Datasets Name | Image Modal | Sample Size | Country | Date | Data Format | Online URL |
|-----------------------------|-------------|---|-------------------------|---------|--------------------|---|
| COVID-chestxray [11] | X-ray | 434 (NCP: 434) | Canada | 2,2020 | JPEG PNG JPG | https://github.com/ieee8023/covid-chestxray-dataset |
| QaTa-Cov19 [14] | X-ray | 6286 (BP: 2760, VP: 1485, Normal: 1579, NCP: 462) | Italy Spain China | 5,2020 | / | / |
| COVID-CXNet [15] | X-ray | 452 (NCP: 452) | Canada | 6,2020 | JPG PNG | https://github.com/armiro/COVID-CXNet |
| Synthetic COVID-19 CXR [16] | X-ray | 21,295 (NCP: 21,295) | / | 10,2020 | JPG | https://github.com/hasibzunair/synthetic-covid-cxr-dataset |

Table 1. Cont.

| Datasets Name | Image Modal | Sample Size | Country | Date | Data Format | Online URL |
|---|-------------|--|-------------------------|---------|---------------|---|
| COVIDGR [17] | X-ray | 852 (Normal: 426, NCP: 426) | Spain | 11,2020 | JPG | https://github.com/ari-dasci/OD-covidgr |
| COVID-19 radiography database [18] | X-ray | 15,153 (NCP: 3616, VP: 1345, Normal: 10,192) | India | 3,2021 | PNG | https://www.kaggle.com/tawsifurrahman/covid19-radiography-database |
| COVID-QU-Ex [19] | X-ray | 13,119 (NCP: 11,956, Pneumonia: 1163) | / | 3,2021 | PNG | https://www.kaggle.com/anasmohammedtahir/covidqu |
| COVID19-DB [20] | X-ray | 1559 (NCP: 225, Normal: 1334) | China | 8,2022 | JPG | / |
| BrixIA COVID-19 [21] | X-ray | 4703 (NCP: 4703) | Italy | 8,2020 | DICOM | https://github.com/BrixIA/Brixia-score-COVID-19 |
| COVIDx-CXR [13] | X-ray | 30,000 (patient: 16,400, X-ray: 30,000) | Canada | 11,2021 | PNG | https://github.com/lindawangg/COVID-Net |
| Balanced Augmented COVID CXR Dataset [22] | X-ray | 30,233 (NCP: 8769, LO: 7662, Normal: 8192, VP: 5410) | India | 11,2022 | PNG | https://www.kaggle.com/tr1gg3rtrash/balanced-augmented-covid-cxr-dataset |
| COVID-CT [12] | CT | 812 (NCP: 349, N-NCP: 463) | China | 3,2020 | PNG JPG | https://github.com/UCSD-AI4H/COVID-CT |
| CC-CCII [23] | CT | 617,775 (NCP, CP, Normal) | China | 4,2020 | JPG PNG | http://ncov-ai.big.ac.cn/download |
| COVID-CT-Seg [24] | CT | 20 (NCP: 20) | China | 4,2020 | DICOM | https://gitee.com/junma11/COVID-19-CT-Seg-Benchmark |
| Yan [25] | CT | 165,667 (patient: 861, CT: 165,667) | China | 4,2020 | / | / |
| MosMedData [26] | CT | 20,685 (patient: 1521, CT: 19,685) | Russia | 4,2020 | NIFIT | https://mosmed.ai/datasets/covid19_1110/ |
| SARS-CoV-2 CT-scan [27] | CT | 2482 (NCP: 1252, N-NCP: 1230) | Brazil | 5,2020 | PNG | https://www.kaggle.com/plameneduardo/sarscov2-ctscan-dataset |
| HKBU_HPML_COVID-19 [28] | CT | 340,190 (NCP: 131,517, CP: 135,038, Normal 73,635) | China | 6,2020 | PNG | https://github.com/HKBU-HPML/HKBU_HPML_COVID-19 |
| HUST-19 [29] | CT | 19,685 (patient: 1521, CT: 19,685) | China | 8,2020 | DICOM JPEG | http://ictcf.biocuckoo.cn/HUST-19.php |
| TCIA [30] | CT | 2724 (patient: 2617, CT: 2724) | China Japan Italy | 8,2020 | / | / |

Table 1. Cont.

| Datasets Name | Image Modal | Sample Size | Country | Date | Data Format | Online URL |
|--|-------------|--|--------------------------------|---------|-------------|---|
| CC-19 [31] | CT | 34,006 | China | 12,2020 | JPG | https://github.com/abdckhanstd/COVID-19 |
| MIDRC-RICORD-1a [32] | CT | 31,856 (NCP: 28,395, N-NCP: 5611) | USA | 12.2020 | DICOM | https://doi.org/10.7937/VTW4-X588 |
| COVIDx-CT [13] | CT | 104,009 (Normal: 8066, NCP: 358, Pneumonia 5538) | China | 9,2020 | PNG | https://github.com/lindawangg/COVID-Net |
| COVID-Net CT-2 [33] | CT | 200,000 | / | 1,2021 | CKPT | https://github.com/haydengunraj/COVIDNet-CT/blob/master/docs/models.md |
| COVIDx CT-2A [13] | CT | 194,922 (CT: 194,922) | China Iran AustraliaEngland | 1,2021 | JPG | https://www.kaggle.com/datasets/hgunraj/covidxct |
| COVIDx CT-2B [13] | CT | 201,103 (CT: 201,103) | China Iran AustraliaEngland | 1,2021 | JPG | https://www.kaggle.com/datasets/hgunraj/covidxct |
| COVID-CS [34] | CT | 145,167 (NCP: 69,626, N-NCP: 75,541) | China | 2,2021 | JPG | https://github.com/yuhuan-wu/JCS |
| COVID-CT-Set [35] | CT | 63,849 (NCP: 15,589, Normal: 48,260) | Iran | 3,2021 | TIFF | https://github.com/mr7495/COVID-CTset |
| COVID-CT-MD [36] | CT | 308 (NCP: 160, CP: 69, Normal: 79) | Iran | 4,2021 | DICOM | https://github.com/ShahinSHH/COVID-CT-MD |
| Cov-Pne-Bac [37] | CT | 1566 (NCP: 631, VP: 417, CP: 518) | Turkey | 1,2022 | JPG | / |
| Large-scale Synthetic COVID-19 CT Dataset [38] | CT | 376,000 | / | 9,2022 | JPG | https://www.kaggle.com/datasets/lee123456789/largescale-synthetic-covid19-ct-dataset |
| BIMCV-COVID19+ [39] | X-ray CT | 23,527 (X-ray 18 840, CT: 6687) | Spain | 6,2020 | / | https://github.com/BIMCV-CSUSP/BIMCV-COVID-19 |
| COVID-19-CT-CXR [40] | X-ray CT | 1590 (CT: 1327, CXR 263) | USA | 11,2020 | / | https://github.com/ncbi-nlp/COVID-19-CT-CXR |

Note: NCP: COVID-19, N-NCP: Non COVID-19, BP: Bacterial pneumonia, VP: Viral pneumonia, /: No information found. All the links are accessed on 13 January 2023.

2.2. Data Enhancement Methods

Data augmentation is the main method to increase the sample size of the dataset, which can alleviate the overfitting phenomenon and improve the generalization ability of the model. This section summarizes the data augmentation methods used for COVID-19 in terms of traditional data augmentation and generative adversarial networks [41], as shown in Figure 5.

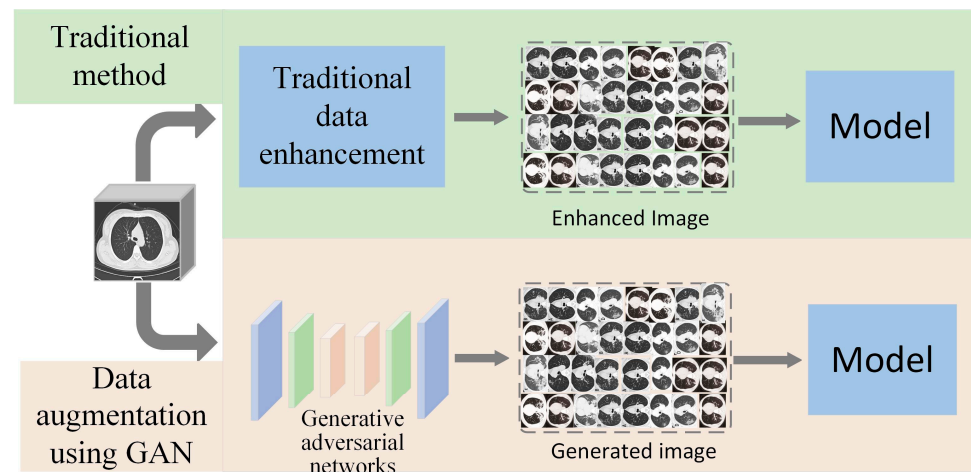


Figure 5. Data augmentation methods.

Traditional data enhancement is the basic way to perform data augmentation, using resizing, scaling, cropping, flipping, and rotating operations to generate the target images. A data augmentation method using generative adversarial networks is a method of generating new data by finding patterns and similarities in the input dataset. Relieving the problem of model overfitting or small samples can be achieved using generative adversarial networks to generate COVID-19 lung images. To generate CT images with stable global structure and diverse local details, Jiang et al. [42] used cGAN to learn global and local information of CT images in generators and discriminators. Waheed et al. [43] proposed ACGAN to generate X-ray images, using the generated data to improve the classification accuracy of original model by 10%. Jiang et al. [44] generated COVID-19 images from lung cancer images with marker information in a CycleGAN model to alleviate the deficiency of high quality marker data and achieve refinement of the model. Barshooi et al. [45] used 8 directional and 8 scale Gabor filters for GAN model to generate X-ray data to improve the quality of image generation. Loey et al. [46] tested combined classical data enhancement and CGAN data generation methods on AlexNet, VGG16, VGG19, GoogleNet and ResNet50, for which ResNet50 model gave the best results.

3. The Methods for Supervised Learning in Diagnosis of COVID-19

The methods for supervised learning in diagnosis of COVID-19 refer to the samples used for model training being labeled. The label information is fully utilized to guide network model training. The advantage is that the model accuracy can be effectively improved by learning a large amount of label information and the model is easy to evaluate. This section summarizes the current state of deep learning for COVID-19 classification and segmentation tasks from aspects of supervised learning, including summarizing the application of VGG, ResNet, DenseNet and lightweight networks to the classification task of COVID-19, and summarizing the application of the attention mechanism, multiscale mechanism, residual connectivity mechanism, and dense connectivity mechanism to the segmentation task of COVID-19.

3.1. The Classification Methods of COVID-19 Based on Supervised Learning

The classification methods of COVID-19 based on supervised learning refers to use of the supervised learning method in extracting features to train a deep network model to distinguish COVID-19. This section focuses on the application to the COVID-19 classification task of VGG, ResNet, DenseNet, and lightweight networks, as shown in Table 2.

Table 2. COVID-19 classification methods based on supervised learning.

| Network Name | Modal | Sample Size | Results (%) | Open Source (Y/N) |
|--------------------|-------------|--|--|-------------------|
| VGG19 [47] | X-ray CT | COVID-19: 4320 Pneumonia: 5856 Normal: 20,000 Lung cancer: 3500 | Acc = 98.05 Recall = 98.05 Auc = 99.66 F1 = 98.24 | Y |
| VGG [48] | X-ray | COVID-19: 5656 Normal: 5656 | Acc = 96.41 Sen = 96.60 Spe = 96.20 Auc = 97.70 | N |
| VGG-16 [49] | X-ray | COVID-19: 816 Pneumonia: 867 Normal: 948 | Acc = 90.00 F1 = 90.00 | N |
| Resnet [37] | CT | COVID-19: 631 VP: 417 BP: 518 | Acc = 99.62 | N |
| FocusCovid [50] | X-ray | / | Acc = 99.40 | |
| ResGANet [51] | CT | COVID-19: 349 Normal: 397 | Acc = 80.00 F1 = 81.00 Auc = 82.00 | N |
| ResGNet-C [52] | CT | COVID-19: 148 Normal: 148 | Acc = 96.62 Sen = 97.33 Spe = 95.91 | N |
| 3D-ResNet [53] | CT | COVID-19: 1315 Pneumonia: 2406 Normal: 936 | Auc = 97.30 | N |
| DenseNet-Tiny [54] | X-ray | COVID-19: 1281 Pneumonia: 4657 Normal: 3270 | Acc = 97.99 Pre = 98.38 Recall = 98.15 F1 = 98.26 | Y |
| DenseNet [55] | X-ray | COVID-19: 2431 Pneumonia: 1468 Normal: 13,649 | Auc = 94.9 Sen = 90.2 Acc = 80.2 | N |
| AM-SdenseNet [56] | CT X-ray | COVID-19:828 Normal:1000 | Acc = 99.18 | Y |
| Corona-Nidnna [57] | X-ray | COVID-19: 245 Pneumonia: 5551 Normal: 8066 | Acc = 95.00 Recall = 94.00 | Y |
| InceptionV3 [58] | X-ray | COVID-19: 162 Pneumonia: 4280 | Acc = 99.96 | N |
| IST-CovNet [1] | CT | COVID-19: 92,905 Pneumonia: 67,712 Normal: 40,030 | Acc = 93.69 | N |
| ML-CAM [59] | X-ray CT | COVID-19: 3254 Normal: 2217 | Acc = 94.72 | N |
| CNN + CFS [60] | CT | COVID-19: 349 Normal: 397 | Acc = 91.60 Sen = 71.70 Pre = 90.40 F1 = 91.00 | N |

Note: /: No information found.

It is not difficult to see the following summary from Table 2. Firstly, the mainstream classification models are based on ResNet in COVID-19. There are three classification models based on VGG, accounting for 18.75%. There are five classification models based on ResNet, accounting for 31.25%. There are three classification models based on DenseNet, accounting for 18.75%. There are five COVID-19 classification models based on lightweight networks, accounting for 31.25%. Secondly, public datasets are mainly used for classification method research on COVID-19. COVID-19 datasets include X-ray datasets, CT datasets and dual-modality datasets that mix X-ray and CT. About 75% of the COVID-19 dataset come from public datasets and 25% of the COVID-19 datasets come from private datasets. Thirdly, regarding the COVID-19 classification, 30% of the tasks are second classification, 46.66% tasks are third classification. Finally, there are relatively few open source and public code resources about the model. The number of public code resources accounted for 25%, and the number of undisclosed code resources accounted for 75%.

3.1.1. The Classification Methods of COVID-19 Based on VGG

VGG [61] is a deep convolutional network structure proposed by Simonyan, which consists of five convolutional blocks and the whole network uses a convolutional kernel of fixed size 3×3 . The first two convolutional blocks use two successive 3×3 convolutional operations and the last three convolutional blocks use three successive 3×3 convolutional operations. The advantage of VGG is its simple structure and easy to perform model improvement. VGG improved model performance by deepening the number of network layers and learning more refined deep network features. The main research work of using VGG as the backbone network for COVID-19 classification task is as follows. Ibrahim et al. [47] used X-ray and CT images in VGG19 to provide complementary information for the classification of COVID-19. Elazab et al. [48] extracted the average of advanced features of infected and healthy cases with the help of pre-trained VGG. The extracted features were used as supervisory signals to retrain VGG to reduce the effect of feature space noise and outliers. Danilov et al. [49] achieved the best results with VGG16 in 10 pre-trained networks by generating attention heat maps to supervise neural networks focusing on the objects in the images.

3.1.2. The Classification Methods of COVID-19 Based on ResNet

ResNet [62] is a convolutional network with residual connection structure proposed in 2015. The feature extraction capability was improved by increasing the depth. However, the gradient disappearance problem leads to a sharp drop in the performance of the model when the network is deepened. The ResNet uses residual connections in the network with the aim of alleviating the gradient disappearance problem in deep neural networks. The residual connections pass the current output directly to the next layer by adding constant mappings between different layers. In the COVID-19 classification task, ResNet is used to alleviate the gradient disappearance problem and improve the classification accuracy of the model. Toğaçar et al. [37] proposed a parallel Resnet network model which uses ResNet-18, ResNet-50, and ResNet-101 to extract different activation sets and improve the classification performance by selecting the dominant activation set. Agrawal et al. [50] added squeezed excitation blocks in residual blocks to enhance lower level feature representation and avoid overfitting by keeping trainable parameters minimal. Cheng et al. [51] improved classification performance by enriching feature information in a single residual block. Yu et al. [52] used the Resnet101 features to underlying relationship between the combined features of graph convolutional neural network to enhance features and improve classification performance. Wang et al. [53] proposed a 3D ResNet-based classification network for COVID-19 in CT images. The residual learning block reduces the complexity of the a priori attention mechanism for transferring the pre-trained detection model.

3.1.3. The Classification Methods of COVID-19 Based on DenseNet

DenseNet [63] is a convolutional network with dense connections structure proposed by Huang Gao. DenseNet connects all the previous layers to the later layers and each layer receives inputs from all the previous layers [64]. Feature reuse is achieved by feature stitching as the input to the next module. The dense connection helps in back propagation of gradients. DenseNet achieves better performance than ResNet in terms of parameters and computational cost. With DenseNet as the backbone network in the COVID-19 classification task, dense connections pass the feature mapping of the current layer to all subsequent layers. The feature reuse approach reduces the number of parameters and alleviates overfitting. Montalbo et al. [54] used DenseNet as a COVID-19 classification network to reduce the number of parameters by reducing the dense network depth increasing the network width. Park et al. [55] proposed a self-attention mechanism based on DenseNet to achieve COVID-19 X-ray image classification by feeding features into transformer. Li et al. [56] applied spatial attention and channel attention to DenseNet, which improved the objective lesion features and suppressed less relevant features to improve the COVID-19 classification accuracy.

3.1.4. The Classification Methods of COVID-19 Based on Lightweight Networks

Methods based on the lightweight COVID-19 classification model refer to minimizing the number of parameters without degrading the model performance. The current lightweight networks mainly include SqueezeNet, ShuffleNet, MobileNet, Inception, etc. The size of model parameters can be effectively compressed by using lightweight networks or by introducing deep separable convolution, group convolution or channel shuffling methods. Lightweight methods have received a lot of attention from researchers. The COVID-19 classification method based on lightweight networks can effectively improve the model training speed and facilitate the deployment on mobile devices. Chakraborty et al. [57] designed a lightweight deep neural network, Corona-Nidaan, which uses deeply separable convolution and multiscale convolution kernels. Das et al. [58] truncated a lightweight network model of InceptionV3 using maximum pooling and global average pooling to reduce the feature dimension, the number of parameters and the complexity of computation [65]. Ahmed et al. [1] added an attention module with a one-dimensional vector representation on Inception-ResNet-V2 to evaluate this convolutional neural network and detect COVID-19 using CT images. Owais et al. [59] integrated complementary feature information through multiple lightweight integrated network models to detect COVID-19 from CT and X-ray images. Abraham et al. [60] proposed an integrated lightweight network that invokes correlated feature selection algorithms in multiple networks of Squeezenet, Darknet-53, MobilenetV2, Xception, and Shufflenet to determine the best subset of features to improve the accuracy.

To sum up, the classification methods of COVID-19 based on VGG use different scales and alternating training methods during the training process, which can converge in fewer epochs and alleviate the training time. There are examples of better transferability and strong generalization ability. However, the VGG COVID-19 classification models use three fully connected layers with too many parameters, which leads to large memory and more computational resources. The classification methods of COVID-19 based on ResNet use residual connections to replicate shallow features directly. The gradient disappearance and network degradation problems are solved by residual connectivity, and the better COVID-19 classification performance is obtained. However, there are more deep layers in ResNet COVID-19 classification model, and it is difficult to optimize; there is a lot of redundant information in this model. The classification methods of COVID-19 based on DenseNet use dense concatenation to transfer shallow layer information directly to the deep layer for further application. The redundancy information is reduced by this model. There are better convergence rates and less parameters at the same network layers. However, when the network layers are increased and features are replicated multiple times, resulting in higher computational complexity and spatial complexity of the model. The classification methods

of COVID-19 based on lightweight networks can reduce the number of parameters and the computation in some degree. There are a few lightweight models which are commonly put into use for mobile devices.

3.2. The Segmentation Methods of COVID-19 Based on Supervised Learning

Image segmentation is an essential task for analyzing medical images and obtaining further diagnostic information in the field of medical image processing. U-net is an image segmentation network structure with classical downsampling and upsampling, which was proposed by Ronnerberger et al. [66]. U-net can obtain accurate segmentation results by employing fewer training samples size. U-net locates COVID-19 lesion regions using deep features and achieves accurate segmentation results using shallow features. This section summarizes the U-net in COVID-19 image segmentation applications combined with attention mechanism, multi-scale mechanism, residual connectivity mechanism and dense connectivity mechanism, as shown in Table 3.

Table 3. COVID-19 segmentation methods based on supervised learning.

| Mechanism | Network Name | Sample Size | Results (%) | Open Source (Y/N) |
|---------------------------------|-------------------------------------|-----------------|---|-------------------|
| Attention mechanism | nCoVSegNet [67] | Slices: 244,537 | Dice = 66.80 ESN = 70.70 SPE = 99.75 PPV = 69.77 | Y |
| Attention mechanism | CAD CNN [68] | Slices: 393 | Dice = 85.43 Recall = 88.10 | N |
| Attention mechanism | D2A U-Net [69] | Slices: 3949 | Dice = 72.98 Recall = 70.71 | N |
| Attention mechanism | DUDA-Net [70] | Slices: 557 | Dice = 87.06 Iou = 77.09 Acc = 99.06 Sen = 90.85 | Y |
| Attention mechanism | RefNet [71] | Slices: 230 | Dice = 91.37 Sen = 91.54 | N |
| Multi-scale mechanism | MSD-Net [72] | Slices: 4780 | Sen = 90.85 Spe = 99.59 | N |
| Multi-scale mechanism | MPS-Net [73] | Slices: 300 | Dice = 83.25 Sen = 84.06 Spe = 99.88 Iou = 74.20 | N |
| Multi-scale mechanism | [74] | Slices: 3929 | Dice = 83.25 Iou = 74.20 | Y |
| Multi-scale mechanism | COVID-SegNet [75] | Slices: 165,667 | Sen = 84.06 Spe = 99.88 | N |
| Multi-scale mechanism | JSC [34] | Slices: 2885 | Dice = 78.50 | Y |
| Residual connectivity mechanism | ResUnet [76] | Slices: 5349 | Dice = 85.19 Sen = 84.66 Prec = 84.22 | Y |
| Residual connectivity mechanism | Backbone + Res_dil + Attention [77] | Slices: 473 | Dice = 83.1 | N |

Table 3. Cont.

| Mechanism | Network Name | Sample Size | Results (%) | Open Source (Y/N) |
|---------------------------------|-------------------|--------------|---|-------------------|
| Residual connectivity mechanism | MultiResUNet [78] | Slices: 3520 | Dice = 74.28 | N |
| Residual connectivity mechanism | Literature [79] | Slices: 100 | Dsc = 94 Acc = 89 Pre = 95 | N |
| Dense connectivity mechanism | SCOAT-Net [80] | Slices: 17 | DSC = 88.99 SEN = 87.85 PPV = 90.28 | N |
| Dense connectivity mechanism | ADID-UNET [81] | Slices: 1318 | Dice = 80.31 Pre = 84.76 Spe = 99.66 Auc = 95.51 | Y |

Note: /: No information found.

It is not difficult to see the following summary from Table 3. Firstly, the methods of U-Net combined with the attention mechanism and U-Net combined with the multiscale mechanism were more often adopted in COVID-19 lesion segmentation. There are five COVID-19 segmentation models based on the attention mechanism, accounting for 31.25% of all the methods of U-Net. There are five COVID-19 segmentation models based on a multi-scale mechanism, accounting for 31.25%. There are four COVID-19 segmentation models based on a residual connection mechanism, accounting for 25%. There are two COVID-19 segmentation models based on the dense connection mechanism, accounting for 12.5%. Secondly, the CT modality datasets are used for all COVID-19 segmentation methods of U-net, and X-ray is rarely used as a segmentation dataset. Thirdly, more COVID-19 segmentation methods focus on research on public datasets which account for 81.81% of all the datasets. Fourthly, there are relatively few open source code resources in terms of the models. The number of public code resources accounted for 37.5%, the number of undisclosed code resources accounted for 62.5%.

3.2.1. The Segmentation Methods of COVID-19 Based on Attention Mechanism

The segmentation methods of COVID-19 based on the attention mechanism refer to calculating its attention distribution based on the input information and obtaining the context vector to selectively focus on the key information of the lesion region in the COVID-19 image. This method can select the information that is more critical to segmentation task among redundant information and improve the segmentation performance by efficiently selecting segmentation features in COVID-19 images. The attention mechanism has received a lot of attention from researchers since it was proposed and the following work has been done in COVID-19 segmentation lesions. Liu et al. [67] used spatial and channel attention in U-Net to segment COVID-19 lung infections. The problem of boundary unclear and lesions complex was solved by making the upper and lower features combined. Karthik et al. [68] introduced contour attention on the last two decoders to refine the infected region for COVID-19 lesion segmentation. The noise inherent in the coarse contour region is discarded by combining shape and boundary information structural features with depth semantic feature maps. Zhao et al. [69] applied gate attention between encoder and decoder to suppress irrelevant information noise and refine the upsampling features. Xie et al. [70] proposed a model based on expansive attention applied between encoder and decoder to solve the redundancy problem in high-level and low-level feature channels. Kitrungrotsakul et al. [71] proposed an interactive attention in U-Net that emphasizes important sensitive segmentation lesions by using residual attention.

3.2.2. The Segmentation Methods of COVID-19 Based on Multi-scale Mechanism

The COVID-19 segmentation method based on the multi-scale mechanism refers to the multi-scale features obtained from receptive field for COVID-19 lesion segmentation. The multiscale feature extraction method reduces the loss of lesion edge and spatial location information and improves segmentation performance by combining multiscale feature receptive field information. Scale invariant features are learned without loss of information to improve the segmentation accuracy of weak lesion and boundary. For the problems of different sizes of COVID-19 lesions, blurred boundaries and the gaps between high and low levels, researchers mainly carried out the following work. Zheng et al. [72] proposed a multiscale discriminative segmentation network, MSD-Net, using pyramidal convolution blocks to achieve multiscale sensory fields for input feature maps. Pei et al. [73] used grouped convolution in an encoder to achieve multiscale feature extraction. Bose et al. [74] proposed a deep multiscale segmentation network, in which the deep multiscale module captures multi-spatial dimensional objects based on acquiring different depth feature maps. Yan et al. [75] proposed a 3D segmentation network, COVID-SegNet, which implicitly enhances the contrast and adaptively adjusts intensity on the feature layer to capture effective features of different scales. Wu et al. [34] enhanced segmentation features by aggregating different scale feature maps from different stages to segment COVID-19 lesions.

3.2.3. The Segmentation Methods of COVID-19 Based on Residual Connectivity Mechanism

The COVID-19 segmentation method based on the residual mechanism refers to a feature pass by using jump connections in the network cross-layer or using residual blocks to replace the convolutional layer for COVID-19 lesions segmentation. This method improves the feature reuse capability by introducing residual mechanism to ensure the back propagation of gradients and alleviate the degradation problem caused by deep networks. Hu et al. [76] proposed a COVID-19 segmentation network using ResUnet as the backbone to reduce the semantic gap between high and low feature maps. Zhou et al. [77] introduced residual connections in COVID-19 lesion segmentation network of U-Net to improve segmentation performance by integrating segmentation information from different levels. Yang et al. [78] reduced the contextual semantic gap by concatenating the outputs of three series of convolutional layers through residual connections in a jump connection structure. Chen et al. [79] captured complex features from the original image to segment COVID-19 lesions by using a topology of residual connections in U-Net to better learn potential representation of the input CT image.

3.2.4. The Segmentation Methods of COVID-19 Based on Dense Connectivity Mechanism

The COVID-19 segmentation method based on the dense connectivity mechanism refers to the use of dense connectivity in the network for interconnection between any layers to achieve feature reuse for COVID-19 lesions segmentation. The use of dense connectivity in the model can reduce the interdependence between different layers and reduce the problem of difficult optimization due to gradient disappearance in the deep network. Zhao et al. [80] proposed a U-Net++ COVID-19 segmentation model, SCOAT-Net, to further reduce semantic gap and produce fine segmentation results by nesting dense jump paths connecting. Raj et al. [81] used two dense networks instead of traditional convolution in U-net networks to enhance global feature propagation, encourage feature reuse and accelerate information transfer to improve segmentation accuracy.

To sum up, there are some advantages in the segmentation methods of COVID-19 based on the attention mechanism, such as ignoring irrelevant feature information, selecting important feature information. However, the COVID-19 segmentation model with added attention mechanism usually has a complex model structure, and it is difficult to find a simple and lightweight segmentation model with an attention mechanism. The segmentation methods of COVID-19 based on multi-scale mechanism are beneficial to obtain the features of different size by combining multi-scale feature receptive fields, and thus improve the

recognition ability of multi-scale target. However, the multi-scale mechanism may lose the continuity features by using different scales of receptive fields. The segmentation methods of COVID-19 based on residual connectivity mechanism are beneficial to speed-up model gradient back propagation. Model training instability is prevented, and gradient disappearance avoided. However, it lacks the ability to explore segmentation feature extraction from the full scale. The segmentation methods of COVID-19 based on dense connectivity mechanism are beneficial to improve the efficiency of feature information transmission, which can better solve the problem of image detail loss and improve the segmentation performance of the network. However, it usually has a complex network structure and a lot of parameters in segmentation model.

4. The Methods for Semi-Supervised Learning in Diagnosis of COVID-19

The semi-supervised learning of COVID-19 images diagnosis method refers to the samples used for model training being only partially labeled. It accomplishes the learning task by training with unlabeled samples and labeled samples together. The advantage is it can improve the accuracy with fewer image labeled samples and alleviate the limitations of small samples labeled in COVID-19 datasets. This section summarizes the application of semi-supervised learning from two aspects, which are COVID-19 images diagnosis application based on the consistent regularization method and COVID-19 images diagnosis application based on the self-training method.

Firstly, the consistency regularization method. Consistent regularization means that the actual perturbation is added to unlabeled data and the output result does not change significantly. In the consistency regularization method, the model is constrained using the corresponding loss function to accomplish a semi-supervised learning task. Li et al. [82] proposed a self-integrating consistent regularization method to mitigate the interference of noisy pseudo labels to each model. The prediction of COVID-19 by moving average index integration of unlabeled data has good performance. Li et al. [83] used a semi-supervised bicoherent learning network in lesion segmentation of COVID-19. Image transformation equivalence was added during training to learn representations of different inputs or feature variants. Ding et al. [84] proposed a consistent time integration model to learn lesion features from noisy annotated CT scans. The model robustness and segmentation performance are improved by introducing noise perception loss in the teacher–student architecture. Abdel et al. [85] implemented knowledge representation interaction between two paths in a semi-supervised COVID-19 lesion segmentation network by feature reorganization to overcome the infection size variation problem. Gan et al. [86] proposed a random combination of data augmentation to improve the diversity of the dataset and the robustness of the semi-supervised network, which can improve performance of COVID-19 images identification.

Secondly, self-training methods. The self-training method is unlike the consistent regularization method and it does not rely on data augmentation. The self-training method determines pseudo labeling by its own model confidence. The self-training method stops training until the model fails to produce the most plausible prediction or all unlabeled data are labeled. Fan et al. [87] provided a self-training based semi-supervised learning to alleviate the shortage unlabeled data. The solution is based on a random choice strategy that uses unlabeled data to gradually expand training dataset. Haque et al. [88] proposed a self-training teacher–student network where the teacher model generates pseudo labels on unlabeled X-ray images. The shortage of COVID-19 datasets is alleviated by training the student model on the labeled and pseudo labeled datasets.

To sum up, the consistency regularization method effectively utilizes the unlabeled data to improve the model performance and alleviate the limitations of the small sample COVID-19 dataset. However, the accuracy and coverage of pseudo label need to be improved. Self-training methods, such as a simple semi-supervised learning method applied to COVID-19 diagnosis, are beneficial to alleviate the problem of the high cost of labeling and difficult label acquisition. The disadvantages are that errors in label

prediction early in the model are reinforced and the model has limitations in terms of convergence.

5. The Methods for Unsupervised Learning in Diagnosis of COVID-19

The unsupervised learning diagnostic method of COVID-19 images is training the model with unlabeled samples and the model learning from the original samples without the help of artificially given labels or feedback as guiding information. This section summarizes the unsupervised learning diagnostic method of COVID-19 in two aspects, which are the autoencoder method from COVID-19 images diagnostic and the unsupervised generative adversarial diagnostic method from COVID-19 images.

Firstly, the COVID-19 images diagnosis method based on autoencoder. Autoencoder is one of the unsupervised learning approaches, which minimizes reconstruction errors by learning valid codes of data. The COVID-19 image diagnosis task can be implemented by learning valid data representations from large-scale unlabeled data. Mansour et al. [89] proposed a novel unsupervised autoencoder network model for COVID-19 classification. Appropriate class labels are assigned to COVID-19 images by adjusting the hyperparameters of the Inceptionv4. Rashid et al. [90] proposed a weight initialization model using unsupervised image reconstruction. It accurately captures the spatial features of the input image and automatically learns features from unlabeled data automatically. Scarpiniti et al. [91] used a deep denoising convolutional autoencoder to transform the classification task into evaluating the difference between the target histogram and the test image histogram. The model improves classification performance while reducing computational cost.

Secondly, an unsupervised generative adversarial diagnostic method from COVID-19 images. Generating adversarial networks is a type of unsupervised learning, which achieves unsupervised deep learning by mapping feature vectors of samples into corresponding labels. The method generates target images by learning the probability distribution of data. Zunair et al. [16] proposed to learn the mapping function between non-COVID-19 images and COVID-19 in an unsupervised learning manner to generate COVID-19 chest X-ray images without the need for paired training samples. Morís et al. [92] combined three complementary CycleGAN architectures to generate a set of synthetic images with appropriate separability, using an unsupervised strategy with oversampling to avoid bias in the classification process and generating a set of synthetic images with appropriate separability.

To sum up, there is strong generalization capability in the COVID-19 images diagnosis method based on autoencoder, which can effectively utilize large-scale unlabeled COVID-19 data. However, the model is weak in expressing the semantic information of images and is not strong in modeling complex information. The unsupervised generative adversarial COVID-19 diagnostic method models can easily learn the distribution of real data without too complex modeling, but there are some disadvantages in GAN, such as training instability, gradient disappearance and pattern collapse.

6. Challenges and Future Work

Currently, the COVID-19 assisted diagnosis system based on deep learning is important for identifying and treating COVID-19. Although deep learning methods have been implemented and work well in COVID-19 diagnosis, there are still many challenges that need to be addressed, as shown in Figure 6. This section summarizes four main aspects, which are dataset aspects, model aspects, COVID-19 variant detection aspects and cross-disciplinary knowledge aspects.

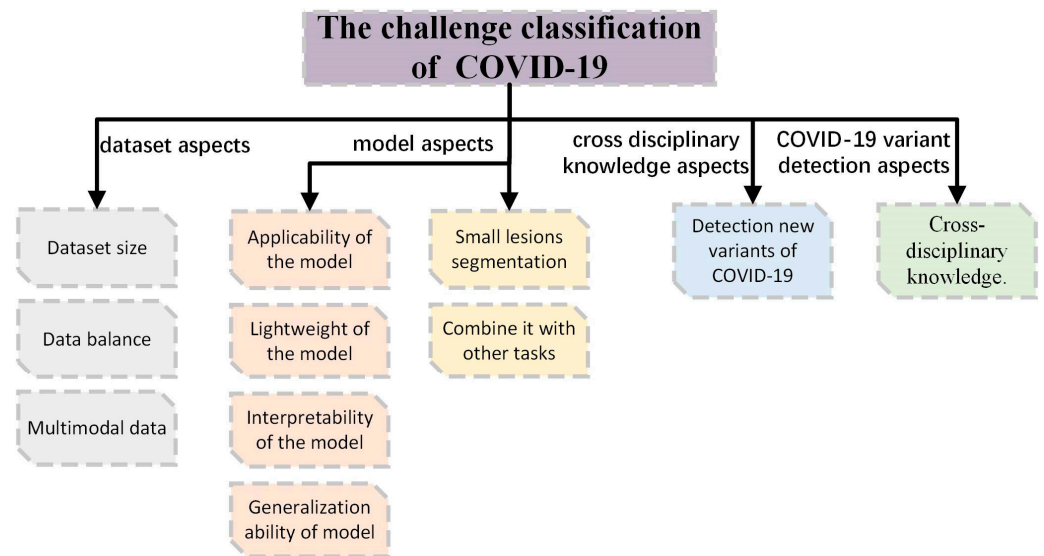


Figure 6. Challenge of diagnostic methods for COVID-19.

First, the dataset aspect mainly includes dataset size, data balance and multimodal data.

Dataset size

The COVID-19 diagnostic methods based on deep learning rely heavily on large datasets, especially different variants of the virus that cannot be easily collected in a short time, and it is essential to build a large public high-quality multiclassification dataset.

Data balance

The COVID-19 diagnostic methods based on deep learning suffer from data imbalance. For example, Chakraborty et al. [57] and Das et al. [58] use datasets with a data imbalance problem, and the model will not learn the best features for accurate classification due to the lack of positive examples. Therefore, effective and verifiable data enhancement techniques are necessary.

Multimodal data

The COVID-19 diagnostic methods based on deep learning mostly use unimodal images; it is also important to use multimodal datasets of COVID-19, such as X-ray and CT images, sound and audio data, and clinical data.

Second, the model aspect mainly includes the challenges faced by classification and segmentation model and the challenges faced by segmentation model. Among them, classification and segmentation models are faced with three challenges, which are applicability of the model, light weight of the model, interpretability of the model and generalization ability of model. The segmentation models are faced with two challenges, which are small target lesions of segmentation and combining with other tasks of segmentation.

Aplicability of the model

Traditional diagnostic methods to identify COVID-19 are a risky process, deep learning method based COVID-19 diagnostics can solve this problem, although many high performance model have been developed, many of them have not been applied to assist in clinical diagnosis. It is a challenge to resolve the applicability issues and apply the deep-learning-based COVID-19 diagnostic method to clinical applications.

Light weight of the model

COVID-19 detection methods mostly focus on the study of non-lightweight models, which are difficult to deploy for smart mobile devices due to the large number of model

parameters. Chakraborty et al. [57] propose a lightweight deep convolutional neural network for COVID-19 cases screening using the chest X-ray samples. The existing lightweight COVID-19 detection models have high requirements for mobile and hardware devices. Therefore, how to lighten the COVID-19 detection model and reduce the requirements of the model for hardware devices is also a hot spot for future research.

Interpretability of the model

COVID-19 diagnostics based on deep learning is an end-to-end highly nonlinear and complex model, and the interpretability of the model is in the initial stage, which brings some obstacles to the application of COVID-19 in real life. Therefore, it is an important research in the future to open the black-box of the deep model and improve the interpretability of the COVID-19 diagnostics model.

Generalization ability of model

Most COVID-19 diagnosis methods based on deep learning are verified by experimental results on a small number of limited dataset, and the results may be biased. In order to compare the experimental results more comprehensively and fairly, it is of great practical value and significance to make multiple experiments on different datasets to verify the generalization ability of the model.

Small lesions segmentation

The segmentation methods of COVID-19 based on supervised learning are shown in Table 2. Performance gains are achieved through a combination of attention mechanism, multi-scale mechanism, residual connectivity mechanism and dense connectivity mechanism. The multi-scale mechanism is used to segment the lesions of different scales. However, the segmentation of small lesions has always been a major difficulty in medical image segmentation. Therefore, it is very important to further study the segmentation of small lesions in COVID-19 segmentation methods based on deep learning.

Combine it with other tasks

Most of the COVID-19 segmentation methods based on deep learning focus on using U-Net as the backbone network, because U-Net shows good performance in medical image segmentation tasks. However, when the network model is faced with some complex segmentation tasks, the performance of the model may be degraded. Therefore, it is an important research direction to realize the multi-task model by combining with other tasks, such as detection before segmentation, and to explore and develop some more advanced multi-task segmentation models to meet the needs of different problems.

Third, detection of new variants of COVID-19

Delta and Omicron are new variants of COVID-19 with a short incubation period, mild symptoms, fast transmission rate and the capability to easily attack patients with low immunity or diseases. How to detect new variants of COVID-19 provides physicians with computer-aided diagnosis as a future research direction.

Fourth, cross disciplinary knowledge

Most researchers have a background in computer science and lack interdisciplinary knowledge; more and more medical science knowledge and expertise are included in deep learning based COVID-19 diagnostic methods. Therefore, the cooperation of experts from multiple disciplines is necessary. There is an urgent need to continuously promote the development of deep-learning-based COVID-19 medical image recognition technology.

7. Conclusions

This paper reviews the recent progress of deep learning in COVID-19 applications from COVID-19 datasets and data enhancement methods, supervised learning in COVID-19 applications of classification methods and segmentation methods, semi-supervised learning in COVID-19 applications and unsupervised learning in COVID-19 applications. The

challenges and future work of deep learning in COVID-19 are discussed and the conclusion is given. The deep learning methods to help physicians improve COVID-19 image diagnostic processing and processing speed make great contributions to the improvement of medical diagnosis. This will greatly promote the progress and development of deep learning methods in COVID-19 image diagnostics.

Author Contributions: Conceptualization, T.Z. and F.L.; methodology, T.Z. and F.L.; investigation, H.L. and C.P.; writing—review and editing, F.L.; Supervision, X.Y.; resources, F.L., T.Z., X.Y. and C.P.; data curation, F.L.; All authors have read and agreed to the published version of the manuscript.

Funding: This work was financially supported by the National Natural Science Foundation of China (grant no.62062003), Natural Science Foundation of Ningxia Province (grant no.2022AAC03149), and Key Research and Development Program of Ningxia (grant no.2020KYQD08).

Institutional Review Board Statement: Not applicable.

Informed Consent Statement: Not applicable.

Data Availability Statement: The data presented in this study are available on request from the corresponding author. The data are not publicly available due to privacy or ethical restrictions.

Acknowledgments: This project was carried out by Tao Zhou's Laboratory of Computer Science and Engineering School of North Minzu University. It was guided and supported by the research direction of Tao Zhou's team from North Minzu University of science and technology. We sincerely thank them for their help in revising the paper.

Conflicts of Interest: The authors declare no conflict of interest.

References

- Ahmed, S.A.A.; Yavuz, M.C.; Şen, M.U.; Gülşen, F.; Tutar, O.; Korkmazer, B. Comparison and ensemble of 2D and 3D approaches for COVID-19 detection in CT images. *Neurocomputing* **2022**, *488*, 457–469. [[CrossRef](#)] [[PubMed](#)]
- WHO Coronavirus (COVID-19) Dashboard. Available online: <https://covid19.who.int/> (accessed on 21 July 2022).
- Gourdeau, D.; Potvin, O.; Archambault, P.; Chartrand-Lefebvre, C.; Dieumegarde, L.; Forghani, R. Tracking and predicting COVID-19 radiological trajectory on chest X-rays using deep learning. *Sci. Rep.* **2022**, *12*, 5616. [[CrossRef](#)]
- Song, L.; Liu, X.; Chen, S.; Liu, S.; Liu, X.; Muhammad, K. A deep fuzzy model for diagnosis of COVID-19 from CT images. *Appl. Soft. Comput.* **2022**, *122*, 108883. [[CrossRef](#)] [[PubMed](#)]
- Yu, G.; Sun, K.; Xu, C.; Shi, X.H.; Wu, C.; Xie, T. Accurate recognition of colorectal cancer with semi-supervised deep learning on pathological images. *Nat. Commun.* **2021**, *12*, 6311. [[CrossRef](#)]
- Wang, X.; Yuan, Y.; Guo, D.; Huang, X.; Cui, Y.; Xia, M. SSA-Net: Spatial self-attention network for COVID-19 pneumonia infection segmentation with semi-supervised few-shot learning. *Med. Image Anal.* **2022**, *79*, 102459. [[CrossRef](#)]
- Chen, H.; Jiang, Y.; Loew, M.; Ko, H. Unsupervised domain adaptation based COVID-19 CT infection segmentation network. *Appl. Intell.* **2022**, *52*, 6340–6353. [[CrossRef](#)] [[PubMed](#)]
- Soomro, T.A.; Zheng, L.; Afifi, A.J.; Ali, A.; Yin, M.; Gao, J. Artificial intelligence (AI) for medical imaging to combat coronavirus disease (COVID-19): A detailed review with direction for future research. *Artif. Intell. Rev.* **2022**, *55*, 1409–1439. [[CrossRef](#)]
- Hassan, H.; Ren, Z.; Zhou, C.; Khan, M.A.; Pan, Y.; Zhao, J.; Huang, B. Supervised and weakly supervised deep learning models for COVID-19 CT diagnosis: A systematic review. *Comput. Meth. Prog. Bio.* **2022**, *218*, 106731. [[CrossRef](#)]
- Subramanian, N.; Elharrouss, O.; Al-Maadeed, S.; Chowdhury, M. A review of deep learning-based detection methods for COVID-19. *Comput. Biol. Med.* **2022**, *143*, 105233. [[CrossRef](#)]
- Cohen, J.P.; Morrison, P.; Dao, L.; Roth, K.; Duong, T.Q.; Ghassemi, M. COVID-19 image data collection: Prospective predictions are the future. *arXiv* **2020**, arXiv:2006.11988.
- Zhao, J.; Zhang, Y.; He, X.; Xie, P. Covid-ct-dataset: A ct scan dataset about COVID-19. *arXiv* **2020**, arXiv:2003.13865.
- Wang, L.; Lin, Z.Q.; Wong, A. Covid-net: A tailored deep convolutional neural network design for detection of COVID-19 cases from chest x-ray images. *Sci. Rep.* **2020**, *10*, 19549. [[CrossRef](#)] [[PubMed](#)]
- Yamac, M.; Ahishali, M.; Degerli, A.; Kiranyaz, S.; Chowdhury, M.E.; Gabbouj, M. Convolutional sparse support estimator-based COVID-19 recognition from X-ray images. *IEEE. Trans. Neural. Netw. Learn. Syst.* **2021**, *32*, 1810–1820. [[CrossRef](#)] [[PubMed](#)]
- Haghanifar, A.; Majdabadi, M.M.; Choi, Y.; Deivalakshmi, S.; Ko, S. Covid-cxnet: Detecting COVID-19 in frontal chest x-ray images using deep learning. *Multimed. Tools Appl.* **2022**, *81*, 30615–30645. [[CrossRef](#)]
- Zunair, H.; Hamza, A.B. Synthesis of COVID-19 chest X-rays using unpaired image-to-image translation. *Soc. Netw. Anal. Min.* **2021**, *11*, 23. [[CrossRef](#)]

17. Tabik, S.; Gómez-Ríos, A.; Martín-Rodríguez, J.L.; Sevillano-García, I.; Rey-Area, M.; Charte, D. COVIDGR dataset and COVID-SDNet methodology for predicting COVID-19 based on chest X-ray images. *IEEE J. Biomed. Health* **2020**, *24*, 3595–3605. [[CrossRef](#)] [[PubMed](#)]
18. Chowdhury, M.E.; Rahman, T.; Khandakar, A.; Mazhar, R.; Kadir, M.A.; Mahbub, Z.B. Can AI help in screening viral and COVID-19 pneumonia? *IEEE Access* **2020**, *8*, 132665–132676. [[CrossRef](#)]
19. COVID-QU-Ex Dataset. Available online: <https://www.kaggle.com/datasets/anasmohammedtahir/covidqu> (accessed on 25 October 2021).
20. Wang, Z.; Xiao, Y.; Li, Y.; Zhang, J.; Lu, F.; Hou, M. Automatically discriminating and localizing COVID-19 from community-acquired pneumonia on chest X-rays. *Pattern Recogn.* **2021**, *110*, 107613. [[CrossRef](#)] [[PubMed](#)]
21. Signoroni, A.; Savardi, M.; Benini, S.; Adami, N.; Leonardi, R.; Gibellini, P. BS-Net: Learning COVID-19 pneumonia severity on a large chest X-ray dataset. *Med. Image Anal.* **2021**, *71*, 102046. [[CrossRef](#)]
22. Roy, S.; Tyagi, M.; Bansal, V.; Jain, V. SVD-CLAHE boosting and balanced loss function for COVID-19 detection from an imbalanced Chest X-Ray dataset. *Comput. Biol. Med.* **2022**, *150*, 106092. [[CrossRef](#)]
23. Zhang, K.; Liu, X.; Shen, J.; Li, Z.; Sang, Y.; Wu, X. Clinically applicable AI system for accurate diagnosis, quantitative measurements, and prognosis of COVID-19 pneumonia using computed tomography. *Cell* **2020**, *181*, 1423–1433. [[CrossRef](#)] [[PubMed](#)]
24. Ma, J.; Wang, Y.; An, X.; Ge, C.; Yu, Z.; Chen, J. Toward data-efficient learning: A benchmark for COVID-19 CT lung and infection segmentation. *Med. Phys.* **2021**, *48*, 1197–1210. [[CrossRef](#)]
25. Yan, Q.; Wang, B.; Gong, D.; Luo, C.; Zhao, W.; Shen, J. COVID-19 chest CT image segmentation—A deep convolutional neural network solution. *arXiv* **2020**, arXiv:2004.10987.
26. Morozov, S.P.; Andreychenko, A.E.; Blokhin, I.A.; Gelezhe, P.B.; Gonchar, A.P.; Nikolaev, A.E. MosMedData: Data set of 1110 chest CT scans performed during the COVID-19 epidemic. *Dig. Diag.* **2020**, *1*, 49–59. [[CrossRef](#)]
27. Soares, E.; Angelov, P.; Biaso, S.; Froes, M.H.; Abe, D.K. SARS-CoV-2 CT-scan dataset: A large dataset of real patients CT scans for SARS-CoV-2 identification. *MedRxiv* **2020**. [[CrossRef](#)]
28. He, X.; Wang, S.; Shi, S.; Chu, X.; Tang, J.; Liu, X. Benchmarking deep learning models and automated model design for COVID-19 detection with chest CT scans. *MedRxiv* **2020**. [[CrossRef](#)]
29. Ning, W.; Lei, S.; Yang, J.; Cao, Y.; Jiang, P.; Yang, Q. Open resource of clinical data from patients with pneumonia for the prediction of COVID-19 outcomes via deep learning. *Nat. Biomed. Eng.* **2020**, *4*, 1197–1207. [[CrossRef](#)]
30. Harmon, S.A.; Sanford, T.H.; Xu, S.; Turkbey, E.B.; Roth, H.; Xu, Z. Artificial intelligence for the detection of COVID-19 pneumonia on chest CT using multinational datasets. *Nat. Commun.* **2020**, *11*, 4080. [[CrossRef](#)]
31. Kumar, R.; Khan, A.A.; Kumar, J.; Golilarz, N.A.; Zhang, S.; Ting, Y. Blockchain-federated-learning and deep learning models for COVID-19 detection using CT imaging. *IEEE Sens. J.* **2021**, *21*, 16301–16314. [[CrossRef](#)]
32. Tsai, E.; Simpson, S.; Lungren, M.P.; Hershman, M.; Roshkovan, L. Medical Imaging Data Resource Center-rsna International COVID Radiology Database Release 1a-Chest ct COVID+ (midrc-ricord-1a). Available online: <https://wiki.cancerimagingarchive.net/x/DoDTB> (accessed on 10 December 2021).
33. Gunraj, H.; Sabri, A.; Koff, D.; Wong, A. COVID-Net CT-2: Enhanced deep neural networks for detection of COVID-19 from chest CT images through bigger, more diverse learning. *Front. Med.* **2022**, *8*, 3126. [[CrossRef](#)]
34. Wu, Y.H.; Gao, S.H.; Mei, J.; Xu, J.; Fan, D.P.; Zhang, R.G. Jcs: An explainable COVID-19 diagnosis system by joint classification and segmentation. *IEEE Trans. Image Process.* **2021**, *30*, 3113–3126. [[CrossRef](#)] [[PubMed](#)]
35. Rahimzadeh, M.; Attar, A.; Sakhaei, S.M. A fully automated deep learning-based network for detecting COVID-19 from a new and large lung ct scan dataset. *Biomed. Signal. Process.* **2021**, *68*, 102588. [[CrossRef](#)]
36. Afshar, P.; Heidarian, S.; Enshaei, N.; Naderkhani, F.; Rafiee, M.J.; Oikonomou, A. COVID-CT-MD, COVID-19 computed tomography scan dataset applicable in machine learning and deep learning. *Sci. Data.* **2021**, *8*, 121. [[CrossRef](#)]
37. Toğaçar, M.; Muzoğlu, N.; Ergen, B.; Yarman, B.S.B.; Halefoğlu, A.M. Detection of COVID-19 findings by the local interpretable model-agnostic explanations method of types-based activations extracted from CNNs. *Biomed. Signal. Process.* **2022**, *71*, 103128. [[CrossRef](#)] [[PubMed](#)]
38. Lee, K.W.; Chin, R.K.Y. Diverse COVID-19 CT Image-to-Image Translation with Stacked Residual Dropout. *Bioengineering* **2022**, *9*, 698. [[CrossRef](#)] [[PubMed](#)]
39. Vayá, M.D.L.I.; Saborit, J.M.; Montell, J.A.; Pertusa, A.; Bustos, A.; Cazorla, M. Bimcv COVID-19+: A large annotated dataset of rx and CT images from COVID-19 patients. *arXiv* **2020**, arXiv:2006.01174.
40. Peng, Y.; Tang, Y.; Lee, S.; Zhu, Y.; Summers, R.M.; Lu, Z. COVID-19-CT-CXR: A freely accessible and weakly labeled chest X-ray and CT image collection on COVID-19 from biomedical literature. *IEEE Trans. Big Data* **2020**, *7*, 3–12. [[CrossRef](#)]
41. Zhou, T.; Li, Q.; Lu, H.; Cheng, Q.; Zhang, X. GAN review: Models and medical image fusion applications. *Inform. Fusion* **2023**, *91*, 134–148. [[CrossRef](#)]
42. Jiang, Y.; Chen, H.; Loew, M.; Ko, H. COVID-19 CT image synthesis with a conditional generative adversarial network. *IEEE J. Biomed. Health* **2020**, *25*, 441–452. [[CrossRef](#)]
43. Waheed, A.; Goyal, M.; Gupta, D.; Khanna, A.; Al-Turjman, F.; Pinheiro, P.R. Covidgan: Data augmentation using auxiliary classifier gan for improved COVID-19 detection. *IEEE Access* **2020**, *8*, 91916–91923. [[CrossRef](#)]

44. Jiang, H.; Tang, S.; Liu, W.; Zhang, Y. Deep learning for COVID-19 chest CT (computed tomography) image analysis: A lesson from lung cancer. *Comput. Struct. Biotech.* **2021**, *19*, 1391–1399. [[CrossRef](#)] [[PubMed](#)]
45. Barshooi, A.H.; Amirkhani, A. A novel data augmentation based on Gabor filter and convolutional deep learning for improving the classification of COVID-19 chest X-Ray images. *Biomed. Signal. Process.* **2022**, *72*, 103326. [[CrossRef](#)] [[PubMed](#)]
46. Loey, M.; Manogaran, G.; Khalifa, N.E.M. A deep transfer learning model with classical data augmentation and CGAN to detect COVID-19 from chest CT radiography digital images. *Neural. Comput. Appl.* **2020**, 1–13. [[CrossRef](#)]
47. Ibrahim, D.M.; Elshennawy, N.M.; Sarhan, A.M. Deep-chest: Multi-classification deep learning model for diagnosing COVID-19, pneumonia, and lung cancer chest diseases. *Comput. Biol. Med.* **2021**, *132*, 104348. [[CrossRef](#)] [[PubMed](#)]
48. Elazab, A.; Abd Elfattah, M.; Zhang, Y. Novel multi-site graph convolutional network with supervision mechanism for COVID-19 diagnosis from X-ray radiographs. *Appl. Soft. Comput.* **2022**, *114*, 108041. [[CrossRef](#)]
49. Danilov, V.V.; Proutski, A.; Karpovsky, A.; Kirpich, A.; Litmanovich, D.; Nefaridze, D. Indirect supervision applied to COVID-19 and pneumonia classification. *Inform. Med. Unlocked* **2022**, *28*, 100835. [[CrossRef](#)]
50. Agrawal, T.; Choudhary, P. FocusCovid: Automated COVID-19 detection using deep learning with chest X-ray images. *Evol. Syst.* **2021**, *13*, 519–533. [[CrossRef](#)]
51. Cheng, J.; Tian, S.; Yu, L.; Gao, C.; Kang, X.; Ma, X. ResGANet: Residual group attention network for medical image classification and segmentation. *Med. Image Anal.* **2022**, *76*, 102313. [[CrossRef](#)]
52. Yu, X.; Lu, S.; Guo, L.; Wang, S.H.; Zhang, Y.D. ResGNet-C: A graph convolutional neural network for detection of COVID-19. *Neurocomputing* **2021**, *452*, 592–605. [[CrossRef](#)]
53. Wang, J.; Bao, Y.; Wen, Y.; Lu, H.; Luo, H.; Xiang, Y. Prior-attention residual learning for more discriminative COVID-19 screening in CT images. *IEEE Trans. Med. Imaging* **2020**, *39*, 2572–2583. [[CrossRef](#)]
54. Montalbo, F.J.P. Diagnosing COVID-19 chest x-rays with a lightweight truncated DenseNet with partial layer freezing and feature fusion. *Biomed. Signal. Process.* **2021**, *68*, 102583. [[CrossRef](#)] [[PubMed](#)]
55. Park, S.; Kim, G.; Oh, Y.; Seo, J.B.; Lee, S.M.; Kim, J.H. Vision transformer using low-level chest X-ray feature corpus for COVID-19 diagnosis and severity quantification. *arXiv* **2021**, arXiv:2104.07235. [[CrossRef](#)]
56. Li, Q.; Ning, J.; Yuan, J.; Xiao, L. A depthwise separable dense convolutional network with convolution block attention module for COVID-19 diagnosis on CT scans. *Comput. Biol. Med.* **2021**, *137*, 104837. [[CrossRef](#)] [[PubMed](#)]
57. Chakraborty, M.; Dhavale, S.V.; Ingole, J. Corona-Nidaan: Lightweight deep convolutional neural network for chest X-Ray based COVID-19 infection detection. *Appl. Intell.* **2021**, *51*, 3026–3043. [[CrossRef](#)] [[PubMed](#)]
58. Das, D.; Santosh, K.C.; Pal, U. Truncated inception net: COVID-19 outbreak screening using chest X-rays. *Phys. Eng. Sci. Med.* **2020**, *43*, 915–925. [[CrossRef](#)] [[PubMed](#)]
59. Owais, M.; Yoon, H.S.; Mahmood, T.; Haider, A.; Sultan, H.; Park, K.R. Light-weighted ensemble network with multilevel activation visualization for robust diagnosis of COVID19 pneumonia from large-scale chest radiographic database. *App. Soft Comput.* **2021**, *108*, 107490. [[CrossRef](#)]
60. Abraham, B.; Nair, M.S. Computer-aided detection of COVID-19 from CT scans using an ensemble of CNNs and KSVM classifier. *Signal Image Video Process.* **2022**, *16*, 587–594. [[CrossRef](#)]
61. Simonyan, K.; Zisserman, A. Very deep convolutional networks for large-scale image recognition. *arXiv* **2014**, arXiv:1409.1556.
62. He, K.; Zhang, X.; Ren, S.; Sun, J. Deep residual learning for image recognition. In Proceedings of the IEEE Conference on Computer Vision and Pattern Recognition, Las Vegas, NV, USA, 25 June–2 July 2016; pp. 770–778.
63. Huang, G.; Liu, Z.; Van Der Maaten, L.; Weinberger, K.Q. Densely connected convolutional networks. In Proceedings of the IEEE Conference on Computer Vision and Pattern Recognition, Honolulu, HI, USA, 16–21 July 2017; pp. 4700–4708.
64. Zhou, T.; Ye, X.; Lu, H.; Zheng, X.; Qiu, S.; Liu, Y. Dense Convolutional Network and Its Application in Medical Image Analysis. *Biomed. Res. Int.* **2022**, *2022*, 2384830. [[CrossRef](#)]
65. Zhou, T.; Chang, X.; Lu, H.; Ye, X.; Liu, Y.; Zheng, X. Pooling Operations in Deep Learning: From “Invariable” to “Variable”. *Biomed. Res. Int.* **2022**, *2022*, 4067581.
66. Ronneberger, O.; Fischer, P.; Brox, T. U-net: Convolutional networks for biomedical image segmentation. In Proceedings of the International Conference on Medical Image Computing and Computer-Assisted Intervention, Munich, Germany, 5–9 October 2015; pp. 234–241.
67. Liu, J.; Dong, B.; Wang, S.; Cui, H.; Fan, D.P.; Ma, J.; Chen, G. COVID-19 lung infection segmentation with a novel two-stage cross-domain transfer learning framework. *Med. Image Anal.* **2021**, *74*, 102205. [[CrossRef](#)]
68. Karthik, R.; Menaka, R.; Hariharan, M.; Won, D. Contour-enhanced attention CNN for CT-based COVID-19 segmentation. *Pattern Recogn.* **2022**, *125*, 108538. [[CrossRef](#)]
69. Zhao, X.; Zhang, P.; Song, F.; Fan, G.; Sun, Y.; Wang, Y. D2A U-net: Automatic segmentation of COVID-19 CT slices based on dual attention and hybrid dilated convolution. *Comput. Biol. Med.* **2021**, *135*, 104526. [[CrossRef](#)]
70. Xie, F.; Huang, Z.; Shi, Z.; Wang, T.; Song, G.; Wang, B.; Liu, Z. DUDA-Net: A double U-shaped dilated attention network for automatic infection area segmentation in COVID-19 lung CT images. *Int. J. Comput. Ass. Rad.* **2021**, *16*, 1425–1434. [[CrossRef](#)]
71. Kitrungratsakul, T.; Chen, Q.; Wu, H.; Iwamoto, Y.; Hu, H.; Zhu, W. Attention-RefNet: Interactive Attention Refinement Network for Infected Area Segmentation of COVID-19. *IEEE J. Biomed. Health* **2021**, *25*, 2363–2373. [[CrossRef](#)]
72. Zheng, B.; Liu, Y.; Zhu, Y.; Yu, F.; Jiang, T.; Yang, D.; Xu, T. MSD-Net: Multi-scale discriminative network for COVID-19 lung infection segmentation on CT. *IEEE Access* **2020**, *8*, 185786–185795. [[CrossRef](#)]

73. Pei, H.Y.; Yang, D.; Liu, G.R.; Lu, T. MPS-net: Multi-point supervised network for CT image segmentation of COVID-19. *IEEE Access* **2021**, *9*, 47144–47153. [[CrossRef](#)] [[PubMed](#)]
74. Bose, S.; Chowdhury, R.S.; Das, R.; Maulik, U. Dense Dilated Deep Multiscale Supervised U-Net for biomedical image segmentation. *Comput. Biol. Med.* **2022**, *143*, 105274. [[CrossRef](#)] [[PubMed](#)]
75. Yan, Q.; Wang, B.; Gong, D.; Luo, C.; Zhao, W.; Shen, J. COVID-19 chest CT image segmentation network by multi-scale fusion and enhancement operations. *IEEE Trans. Big Data* **2021**, *7*, 13–24. [[CrossRef](#)]
76. Hu, H.; Shen, L.; Guan, Q.; Li, X.; Zhou, Q.; Ruan, S. Deep co-supervision and attention fusion strategy for automatic COVID-19 lung infection segmentation on CT images. *Pattern Recogn.* **2022**, *124*, 108452. [[CrossRef](#)] [[PubMed](#)]
77. Zhou, T.; Canu, S.; Ruan, S. Automatic COVID-19 CT segmentation using U-Net integrated spatial and channel attention mechanism. *Int. J. Imag. Syst. Tech.* **2021**, *31*, 16–27. [[CrossRef](#)]
78. Yang, Q.; Li, Y.; Zhang, M.; Wang, T.; Yan, F.; Xie, C. Automatic Segmentation of COVID-19 CT Images Using Improved MultiResUNet. In Proceedings of the 2020 Chinese Automation Congress, Shanghai, China, 6–8 November 2020; pp. 1614–1618.
79. Chen, X.; Yao, L.; Zhang, Y. Residual attention u-net for automated multi-class segmentation of COVID-19 chest CT images. *arXiv* **2020**, arXiv:2004.05645.
80. Zhao, S.; Li, Z.; Chen, Y.; Zhao, W.; Xie, X.; Liu, J. SCOAT-Net: A novel network for segmenting COVID-19 lung opacification from CT images. *Pattern Recogn.* **2021**, *119*, 108109. [[CrossRef](#)] [[PubMed](#)]
81. Raj, A.N.J.; Zhu, H.; Khan, A.; Zhuang, Z.; Yang, Z.; Mahesh, V.G.; Karthik, G. ADID-UNET—A segmentation model for COVID-19 infection from lung CT scans. *PeerJ Comput. Sci.* **2021**, *7*, e349.
82. Li, C.; Dong, L.; Dou, Q.; Lin, F.; Zhang, K.; Feng, Z. Self-Ensembling Co-Training Framework for Semi-Supervised COVID-19 CT Segmentation. *IEEE J. Biomed. Health* **2021**, *25*, 4140–4151. [[CrossRef](#)]
83. Li, Y.; Luo, L.; Lin, H.; Chen, H.; Heng, P.A. Dual-consistency semi-supervised learning with uncertainty quantification for COVID-19 lesion segmentation from CT images. In Proceedings of the International Conference on Medical Image Computing and Computer-Assisted Intervention, Strasbourg, France, 27 September–1 October 2021; Springer: Cham, Switzerland, 2021; pp. 199–209.
84. Ding, W.; Abdel-Basset, M.; Hawash, H. RCTE: A reliable and consistent temporal-ensembling framework for semi-supervised segmentation of COVID-19 lesions. *Inf. Sci.* **2021**, *578*, 559–573. [[CrossRef](#)]
85. Abdel-Basset, M.; Chang, V.; Hawash, H.; Chakraborty, R.K.; Ryan, M. FSS-2019-nCov: A deep learning architecture for semi-supervised few-shot segmentation of COVID-19 infection. *Knowl. Based Syst.* **2021**, *212*, 106647. [[CrossRef](#)] [[PubMed](#)]
86. Gan, Y.; Zhu, H.; Guo, W.; Xu, G.; Zou, G. Deep semi-supervised learning with contrastive learning and partial label propagation for image data. *Knowl. Based Syst.* **2022**, *245*, 108602. [[CrossRef](#)]
87. Fan, D.P.; Zhou, T.; Ji, G.P.; Zhou, Y.; Chen, G.; Fu, H. Inf-net: Automatic COVID-19 lung infection segmentation from CT images. *IEEE Trans. Med. Imaging* **2020**, *39*, 2626–2637. [[CrossRef](#)]
88. Haque, S.; Hoque, M.A.; Khan, M.A.I.; Ahmed, S. COVID-19 Detection Using Feature Extraction and Semi-Supervised Learning from Chest X-ray Images. In Proceedings of the 2021 IEEE Region 10 Symposium, Jeju, Korea, 23–25 August 2021; pp. 1–5.
89. Mansour, R.F.; Escorcia-Gutierrez, J.; Gamarra, M.; Gupta, D.; Castillo, O.; Kumar, S. Unsupervised deep learning based variational autoencoder model for COVID-19 diagnosis and classification. *Pattern Recogn. Lett.* **2021**, *151*, 267–274. [[CrossRef](#)] [[PubMed](#)]
90. Rashid, N.; Hossain, M.A.F.; Ali, M.; Sukanya, M.I.; Mahmud, T.; Fattah, S.A. AutoCovNet: Unsupervised feature learning using autoencoder and feature merging for detection of COVID-19 from chest X-ray images. *Biocybern. Biomed. Eng.* **2021**, *41*, 1685–1701. [[CrossRef](#)] [[PubMed](#)]
91. Scarpiniti, M.; Ahrabi, S.S.; Baccarelli, E.; Piazzo, L.; Momenzadeh, A. A novel unsupervised approach based on the hidden features of Deep Denoising Autoencoders for COVID-19 disease detection. *Expert Syst. Appl.* **2022**, *192*, 116366. [[CrossRef](#)] [[PubMed](#)]
92. Morís, D.I.; de Moura, J.; Novo, J.; Ortega, M. Cycle generative adversarial network approaches to produce novel portable chest X-rays images for COVID-19 diagnosis. In Proceedings of the ICASSP 2021—2021 IEEE International Conference on Acoustics, Speech and Signal Processing, Toronto, ON, Canada, 6–12 June 2021; pp. 1060–1064.

Disclaimer/Publisher’s Note: The statements, opinions and data contained in all publications are solely those of the individual author(s) and contributor(s) and not of MDPI and/or the editor(s). MDPI and/or the editor(s) disclaim responsibility for any injury to people or property resulting from any ideas, methods, instructions or products referred to in the content.